Neurobiology of Stress 14 (2021) 100326

Contents lists available at ScienceDirect

Neurobiology of Stress

journal homepage: www.elsevier.com/locate/ynstr

Alterations of frontal-temporal gray matter volume associate with clinical measures of older adults with COVID-19

Kuaikuai Duan [a,b,*], Enrico Premi [c,d], Andrea Pilotto [d], Viviana Cristillo [d], Alberto Benussi [d], Ilenia Libri [d], Marcello Giunta [d], H. Jeremy Bockholt [b], Jingyu Liu [b,e], Riccardo Campora [f], Alessandro Pezzini [d], Roberto Gasparotti [f], Mauro Magoni [c], Alessandro Padovani [d], Vince D. Calhoun [a,b,e,g]

[a] Department of Electrical and Computer Engineering, Georgia Institute of Technology, Atlanta, USA
[b] Tri-Institutional Center for Translational Research in Neuroimaging and Data Science (TReNDS), Georgia Institute of Technology, Georgia State University, Emory University, Atlanta, USA
[c] Stroke Unit, Azienda Socio Sanitaria Territoriale Spedali Civili, Spedali Civili Hospital, Brescia, Italy
[d] Neurology Unit, Department of Clinical and Experimental Sciences, University of Brescia, Italy
[e] Department of Computer Science, Georgia State University, Atlanta, USA
[f] Neuroradiology Unit, Department of Medical and Surgical Specialties, Radiological Sciences and Public Health, University of Brescia and ASST Spedali Civili Hospital, Brescia, Italy
[g] Department of Psychology, Computer Science, Neurosciences, Mathematics & Statistics, Georgia State University, Atlanta, USA

ARTICLE INFO

Keywords:
COVID-19
Computed tomography
Gray matter volume
Frontal-temporal network
Source-based morphometry

ABSTRACT

COVID-19, the infectious disease caused by the most recently discovered severe acute respiratory syndrome coronavirus-2 (SARS-CoV-2), has become a global pandemic. It dramatically affects people's health and daily life. Neurological complications are increasingly documented for patients with COVID-19. However, the effect of COVID-19 on the brain is less studied, and existing quantitative neuroimaging analyses of COVID-19 were mainly based on the univariate voxel-based morphometry analysis (VBM) that requires corrections for a large number of tests for statistical significance, multivariate approaches that can reduce the number of tests to be corrected have not been applied to study COVID-19 effect on the brain yet. In this study, we leveraged source-based morphometry (SBM) analysis, a multivariate extension of VBM, to identify changes derived from computed tomography scans in covarying gray matter volume patterns underlying COVID-19 in 120 neurological patients (including 58 cases with COVID-19 and 62 patients without COVID-19 matched for age, gender and diseases). SBM identified that lower gray matter volume (GMV) in superior/medial/middle frontal gyri was significantly associated with a higher level of disability (modified Rankin Scale) at both discharge and six months follow-up phases even when controlling for cerebrovascular diseases. GMV in superior/medial/middle frontal gyri was also significantly reduced in patients receiving oxygen therapy compared to patients not receiving oxygen therapy. Patients with fever presented significant GMV reduction in inferior/middle temporal gyri and fusiform gyrus compared to patients without fever. Patients with agitation showed GMV reduction in superior/medial/middle frontal gyri compared to patients without agitation. Patients with COVID-19 showed no significant GMV differences from patients without COVID-19 in any brain region. Results suggest that COVID-19 may affect the frontal-temporal network in a secondary manner through fever or lack of oxygen.

1. Introduction

Coronavirus disease 2019 (COVID-19) continues to affect people's health and daily life. Besides the most characterized symptoms such as fever, cough, fatigue, dyspnea, and headache (Kooraki et al., 2020; Tian et al., 2020), neurologic complications have been increasingly reported in COVID-19. The most frequently reported neurological complications are impaired consciousness, confusion, and agitation, which were more common in severe patients (Helms et al., 2020; Kremer et al., 2020; Lovell et al., 2020; Mao et al., 2020; Moro et al., 2020). Some COVID-19

* Corresponding author. TReNDS Center, 55 Park Place NE, 18th floor, Atlanta, GA, 30303, USA.
E-mail address: kduan30@gatech.edu (K. Duan).

https://doi.org/10.1016/j.ynstr.2021.100326
Received 4 February 2021; Received in revised form 3 April 2021; Accepted 5 April 2021
Available online 13 April 2021

patients also developed encephalopathy (Benussi et al., 2020; Espinosa et al., 2020; Filatov et al., 2020; Pilotto et al., 2020; Benussi et al., 2021; Pilotto et al., 2021), seizure (Asadi-Pooya 2020; Sohal and Mansur 2020), anosmia, and dysgeusia (Agyeman et al., 2020; Carrillo-Larco and Altez-Fernandez, 2020; Wong et al., 2020; Xydakis et al., 2020), which may be caused by the invasion of the virus in the central and peripheral nervous systems (Asadi-Pooya and Simani 2020; Moriguchi et al., 2020; Paniz-Mondolfi et al., 2020; Pezzini and Padovani 2020; Puelles et al., 2020, Yavarpour-Bali and Ghasemi-Kasman, 2020). Recently, direct invasion of the virus in the central nervous system was reported in an animal study (Kumari et al., 2021), where mice presented a much higher amount of SARS-CoV-2 virus in the brains than in the lungs.

Neuroimaging data provide us a good opportunity to study links between COVID-19 and the central nervous system. However, to date, only a few studies have examined the effect of COVID-19 on the brain, and previous findings are inconsistent. Egbert and colleagues (Egbert et al., 2020) summarized that about a third of COVID-19 patients with neuroimaging in the acute/subacute phase presented brain abnormalities, where cerebral white matter hyperintensities (derived from magnetic resonance imaging, MRI)/hypodensities (derived from computed tomography, CT) are the primary manifestation, and these abnormalities were spread across cerebral hemispheres rather than occurring in focal regions. Kandemirli and colleagues (Kandemirli et al., 2020) reported that among 27 adult COVID-19 patients in the intensive care unit, ten presented MRI signal intensity abnormalities, and these abnormalities were located in multifocal brain regions, including frontal, parietal, occipital, and temporal lobes, insular cortex, and cingulate gyrus. A more recent and comprehensive review paper (Choi and Lee 2020) revealed that acute/subacute infarcts were the most prevalent neurological complications of COVID-19, followed by cerebral microhemorrhages, spontaneous intracranial hemorrhage, and encephalitis/encephalopathy, in line with clinical evidence based on consecutive subjects evaluated for neurological alterations in acute settings (Frontera et al., 2020; Pilotto et al., 2021). Kremer et al. (Kremer et al., 2020) investigated brain abnormalities in 37 severe COVID-19 patients without ischemic infarcts. They reported that the most frequent MRI characteristic were signal abnormalities in the medial temporal lobe (43%), followed by nonconfluent multifocal white matter hyperintense lesions on fluid-attenuated inversion recovery images with variable enhancement and hemorrhagic lesions (30%), and extensive and isolated white matter microhemorrhages (24%). However, most of the aforementioned studies were based on experienced neurologists' visual assessment. This qualitative approach does not scale and may not be reproducible across patients and sites and does not provide detailed and quantified information about changes in brain patterns.

In contrast, automated data-driven approaches can quantify changes in brain patterns across participants with much less time, and the identified patterns were more reproducible compared to that from qualitative approaches. However, analytical neuroimaging studies of COVID-19 are still rare. Lu et al. (Lu et al., 2020) examined the difference of gray (derived from structural MRI)/white (derived from diffusion tensor imaging (DTI)) matter volume between 60 recovered COVID-19 patients and 39 controls at a three-month follow-up by conducting voxel-based morphometry (VBM) and atlas-based analyses. They reported that recovered COVID-19 patients presented higher gray matter volume (GMV) in widespread brain regions such as olfactory cortices, hippocampi, insulas, and right cingulate gyrus, lower mean, axial and radial diffusivities, as well as higher fractional anisotropy. Some of these brain regions and global GMV were related to COVID-19 related clinical measurements. More recently, Crunfli and colleagues (Crunfli et al., 2020) conducted a cortical surface-based morphometric analysis on MRI scans of 145 healthy controls and 81 COVID-19 patients that had mild respiratory symptoms. They revealed that COVID-19 patients demonstrated reduced cortical thickness in the left lingual gyrus, calcarine sulcus, and olfactory sulcus and increased cortical thickness in the precentral and postcentral gyrus, and superior occipital gyrus. Another surface-based morphometric study (Salomon et al., 2020) showed that the lockdown remedy for slowing down COVID-19 spread affected the brain structure of 50 healthy individuals in Israel (T1-weighted MRI were obtained prior to the outbreak and after the lockdown period), which introduced increased GMV in bilateral amygdala, putamen, and the anterior temporal cortices, and GMV increase in the amygdala diminished as time elapsed from lockdown alleviation. Current analytical neuroimaging studies examining structural changes introduced by COVID-19 mainly focus on structural MRI and DTI data, considering regions of interest (ROIs) of the involved brain defined by different atlases or whole brain based on univariate VBM analyses. Other data modalities (for example, CT) and multivariate approaches (for example, multivariate source-based morphometry (Xu et al., 2009)) have not yet been applied to study COVID-19.

To further study patterns of gray matter change, we investigate GMV alterations underlying COVID-19 in a cohort of 120 older adults (58 COVID-19 patients and 62 non-COVID-19 participants) by applying source-based morphometry (SBM (Xu et al., 2009)) to GMV data derived from CT images. SBM is a multivariate blind source separation method to capture covarying patterns of GMV among individuals. SBM assumes GMV sources are statistically independent and enables source-level analysis, which reduces the number of tests to be corrected and further boosts the statistical power. Moreover, we compare SBM results with results from univariate VBM to further evaluate the main findings. To our best knowledge, this is the first study to investigate CT-derived GMV alterations underlying COVID-19 by using a multivariate analytical approach.

2. Materials and methods

2.1. Participants

The observational study included consecutive patients evaluated for neurological symptoms at the Hospital "Azienda Socio Sanitaria Territoriale Spedali Civili", Brescia, Italy. The Hospital is located in a metropolitan area of more than 1,200,000 people and hosted the greatest number of admitted COVID-19 patients in Italy to date (Padovani 2020). Since March 8th, most hospitals were transformed into COVID Hospitals and neurological units were closed, but the Neurology Department of the ASST-Spedali Civili Hospital was designated as a hub for neurological disorders including stroke and established a dedicated Special Neuro-COVID Acute Unit during the COVID-19 outbreak. The study was approved by the local ethics committee of the ASST Spedali Civili di Brescia Hospital and the requirement for informed consent was waived by the Ethics Commission (NP 4067, approved 08.05.2020) (Pilotto et al., 2020).

2.2. Data collection and clinical measurements

Epidemiological, demographical, clinical, laboratory, treatment, and outcome data were extracted from both printed and electronic medical records using standardized anonymized data collection forms. All data were imputed and checked by four physicians (AB, AP, MG, and IL). The admission data of included patients ranged from February 21 to April 5, 2020 (Benussi et al., 2020).

Our study enrolled all adult inpatients who were hospitalized for neurological diseases and had a definite outcome (discharged home or to a rehabilitation facility, or death). The criteria for discharge for patients with COVID-19 were an absence of fever for at least 24 hours, a respiratory rate <22/min, and substantial improvement at chest x-ray or CT scan. SARS-CoV-2 detection in respiratory specimens was performed by real-time RT PCR methods; nasopharyngeal and oropharyngeal swabs were performed in all patients. If two consecutive tests obtained at least 24 hours apart resulted negative, and there was a high suspicion of COVID-19 (i.e., interstitial pneumonia at chest x-ray, the low arterial

partial pressure of oxygen), bronchoalveolar lavage was performed.

Clinical condition scales were assessed, including the quick sequential organ failure assessment (qSOFA) score, the Glasgow Coma Scale (GCS), and the Modified Rankin Scale (mRS) (a 6-point disability scale, the larger the value, the more severe the disability (Wilson et al., 2002)). The mRS was evaluated pre-admission, at discharge, and at 6-month follow-up. Patients were further grouped as having a good/bad outcome based on their mRS scores at discharge (mRS scores in the range of [0, 2]: good outcome; mRS scores in the range of [3, 6]: bad outcome) (Weisscher et al., 2008). COVID-19 symptoms, such as (i) the severity of COVID-19 disease classified according to the Brescia-COVID Respiratory Severity Scale (BCRSS) to stratify patients into mild, moderate, and severe levels (Piva et al., 2020). BCRSS ranges from 0 to 3 and with larger values indicating severe COVID-19 symptom; (ii) diagnosis of pneumonia, fever, respiratory rate; (iii) treatments including oxygen therapy and antibiotic/antiviral treatment, (iv) neurological complications including cerebrovascular events and agitation (an emotion that is more likely to show up when an individual is under intense stress), and (v) diagnosis of diabetes and hypertension, were also collected. Note, fever and receipt of oxygen therapy happened roughly at the time of CT scan.

2.3. CT images and preprocessing

CT images were collected 1–17 (4.5 ± 3.34) days following COVID-19 onsite and were acquired at the same site with two scanners: 1) Aquilon Prime, Toshiba (Toshiba Medical Systems, Tokyo, Japan), slice thickness = 5 mm, kilovoltage peak (KVp) = 120, pixel size (mm): 0.43 x 0.43; 2) Somatom Definition Edge, Siemens (Siemens, Erlangen, Germany), slice thickness = 5 mm, kilovoltage peak (KVp) = 120, pixel size (mm): 0.52 x 0.52.

All included CT images were downsampled to 1 mm × 1 mm x 1 mm and jointly normalized into Montreal Neurological Institute (MNI) space and segmented into six types of tissues (gray matter (GM), white matter, cerebrospinal fluid, skull, soft tissue, and background) using the CTseg toolbox (https://github.com/WCHN/CTseg (Brudfors 2020; Brudfors et al., 2020)). The CTseg toolbox is an extension of the popular unified segmentation routine in SPM 12 (https://www.fil.ion.ucl.ac.uk/spm/software/spm12/ (Penny et al., 2011)), which leveraged priors on the Gaussian mixture model parameters and an atlas learned from both magnetic resonance imaging (MRI) and CT data to yield improved registration and more robust segmentation. Normalized GM images were then modulated and smoothed with a $10 \times 10 \times 10$ mm^3 Gaussian kernel. Further quality control was performed to retain participants with a correlation larger than 0.9 with the mean GM map (no samples were removed for this procedure since all samples had a correlation value larger than 0.9 with the mean GM map). Gray matter refinement (i.e., masking) selected voxels with mean GMV larger than 0.2, yielding 1, 607,344 voxels for further analyses. Total GMV was approximated as the sum of voxel values in the masked GM images for each participant.

2.4. Source-based morphometry analysis on GMV data

We employed SBM, a multivariate extension of VBM built into the GIFT toolbox (http://trendscenter.org/software/gift), to identify maximally independent GMV spatial patterns that covary among individuals. SBM leverages the multivariate blind source separation approach, independent component analysis (ICA) (Bell and Sejnowski 1995), to decompose 120 subjects GMV data into a component matrix and a loading matrix, where the independence of components/sources was maximized (Xu et al., 2009). Each row of the component matrix is one independent component, and values in one component reflect contributions of individual variables (voxels) to the component. Each column of the loading matrix is the loading vector, and values of the loading vector represent expression levels of the corresponding component across participants. The component number was estimated to be 15 based on the minimum description length principle (Rissanen 1978, 1983; Calhoun et al., 2001; Li et al., 2007). Subject-wise mean removal and principal component analysis were employed prior to ICA. ICASSO (Himberg et al., 2004) with 10 ICA runs was used to guarantee a stable decomposition, and the run with the highest stability index was selected as the final ICA decomposition.

2.5. Statistical inference

The loading parameters of the 15 independent GMV components and total GMV were further examined for their ability to discriminate COVID-19 patients from participants without COVID-19 by using the regression model:

Loadings of a GMV component/total GMV = diagnosis (COVID-19/non-COVID-19) + age + gender.

Moreover, the associations between loadings of 15 GMV components and clinical measures showing significant COVID-19 vs. non-COVID-19 difference were tested with the regression model:

Loadings of a GMV component = a clinical measure + diagnosis (COVID-19/non-COVID-19) + age + gender.

Results were corrected for multiple comparisons using a microarray experiments-adjusted false discovery rate (MAFDR (Storey and Tibshirani 2003)) of $p < 0.05$. MAFDR can take dependencies among tested dependent variables into account while measuring the probability of significance. Confounding effects from the cerebral vascular event, diabetes, and hypertension were examined by treating each of them as a covariate separately.

The previous study (Chen et al., 2014) has shown that scanner/site effect can be identified and corrected by SBM, and SBM correction provided more flexibility and ability to handle collinear effects than general linear model-based correction. Thus, in this study, the scanner effect was corrected on SBM results (loadings of components) by adding scanner allocation into the abovementioned models.

2.6. Voxel-based morphometry analysis on GMV data

To further evaluate the results, we performed a univariate analysis, VBM, on the same preprocessed GMV data to identify GM regions discriminating COVID-19 patients from individuals without COVID-19 by using a similar regression model: a GM voxel = diagnosis (COVID-19/non-COVID-19) + age + gender. Similarly, associations between each voxel and COVID-19 discriminative clinical measures were examined using the regression model: a GM voxel = a clinical measure + diagnosis (COVID-19/non-COVID-19) + age + gender. Multiple comparisons were corrected at FDR $p < 0.05$.

2.7. mRS prediction based on identified GMV loadings and clinical variables

We examined the ability of identified GMV components for mRS prediction. Specifically, we used the loadings of identified GMV components (we called it CT model) to predict mRS score at discharge and 6-month follow-up by employing support vector regression (SVR) with the least absolute shrinkage and selection operator (LASSO) regularization. SVR with LASSO can select features of importance and yield stable results. SVR with LASSO was cross-validated with the leave-one-out strategy on the training samples. Regularization parameter λ producing the smallest mean square error among all leave-one-out trials was selected, which was applied to all training samples to generate the final model. The finalized model was applied to the hold-out testing set to evaluate its performance. The performance measures included mean square error (MSE) and correlation coefficient (r) between the predicted mRS and true mRS scores.

In this study, 84 (70% samples) out of 120 patients were used for training, and the remaining 36 (30% samples) were for testing. Beyond identified GMV loadings, clinical and demographic variables, including COVID-19 diagnosis, fever status, receipt of oxygen therapy, hypertension, cerebrovascular event, diabetes, age, and gender (we named it as CT + clinic model), were also tested for mRS prediction.

3. Results

3.1. Summary of demographic and clinical measures

CT scans from fifty-eight adults with COVID-19 (28 female, age: 73.41 ± 10.95) and sixty-two adults without COVID-19 (30 female, age: 69.46 ± 16.62) were analyzed in this study (see Table 1 for detailed demographic information, clinical diagnosis, and outcomes (disability)). For each variable in Table 1, the *p* value and effect size (Chi-square or t statistic value) reflecting COVID-19 vs. non-COVID-19 difference were computed using the Chi-square test (for categorical variables) or two-sample *t*-test (for continuous variables) (the same for Table 2).

Age and female vs. male ratio were comparable between the COVID-19 group and non-COVID-19 group (*p* values of COVID-19 vs. non-COVID-19 difference were larger than 0.05). The clinical diagnosis was relatively balanced between the COVID-19 group and the non-COVID-19 group. Among 120 included participants, 66 were with normal CT (without apparent vascular lesions). 33 out of these 66 individuals were COVID-19 patients.

Table 1
Demographic information, clinical diagnosis and outcome measures.

Total (N = 120)	COVID-19 patients (n = 58)	Non-COVID-19 participants (n = 62)	p value	Effect size
Age (mean ± std)	73.41 ± 10.95	69.46 ± 16.62	0.13	t(118) = 1.52
Gender (Female/Male)	28/30	30/32	0.99	$\chi^2(1) = 1.48 \times 10^{-4}$
Scanner (Siemens/Toshiba)	28/30	26/36	0.49	$\chi^2(1) = 0.49$
Clinical diagnosis				
Brain tumor, (n)	0	2	NA	NA
Encephalopathy, (n)	10	8		
Epilepsy, (n)	7	12		
Headache, (n)	1	3		
ICH, (n)	4	7		
Peripheral nerves alterations, (n)	2	3		
SAH, (n)	2	1		
Stroke, (n)	27	24		
TIA, (n)	5	2		
Disability				
mRS pre admission (mean ± std)	1.19 ± 1.05	1.26 ± 1.31	0.75	t(118) = -0.31
mRS at discharge (mean ± std)	**3.78 ± 2.06**	**2.34 ± 1.66**	**4.81×10^{-5}**	**t(118)= 4.22**
mRS at 6 months (mean ± std)	**3.79 ± 2.08**	**2.23 ± 1.79**	**2.03×10^{-5}**	**t(118)= 4.44**
Outcome (dead/discharged)	**21/37**	**3/59**	**1.76×10^{-5}**	**$\chi^2(1)$= 18.43**
Good outcome (yes/no)	**18/40**	**36/26**	**2.94×10^{-3}**	**$\chi^2(1)$= 8.85**

Note, the *p* value and effect size are for COVID-19 vs. non-COVID-19 difference. χ^2 and *t* denote chi-square and *t* statistic values with degree of freedom inside the parentheses (the same for Table 2), respectively. The Chi-square statistic was not available (NA) for clinical diagnosis since it does not satisfy the assumptions of the Chi-square test. Rows in bold are outcome measures showing significant COVID-19 vs. non-COVID-19 difference (corrected for 5 tests). **Abbreviations:** ICH, intracerebral Hemorrhage; mRS, modified Ranking Scale; SAH, Subarachnoid Hemorrhage; TIA, Transient Ischemic Attack; DF, degree of freedom; std, standard deviation.

Table 2
COVID-19 symptoms and treatment, its neurological complications, and confounding variables.

Total (N = 120)	COVID-19 patients (n = 58)	Non-COVID-19 participants (n = 62)	p value	Effect size
COVID-19 symptoms and treatments				
BCRSS (0/1/2/3)	4/28/19/7	NA	NA	NA
Pneumonia (0/1)	**10/48**	**60/2**	**1.04×10^{-18}**	**$\chi^2(1)$= 77.99**
Respiratory rate>21 (yes/no)	**11/47**	**1/61**	**1.54×10^{-3}**	**$\chi^2(1)$= 10.03**
Fever (yes/no)	**29/29**	**9/53**	**2.97×10^{-5}**	**$\chi^2(1)$= 17.44**
GCS<15 (yes/no)	38/20	35/27	0.31	$\chi^2(1) = 1.03$
Oxygen therapy (yes/no)	**40/18**	**11/51**	**1.41×10^{-8}**	**$\chi^2(1)$= 32.18**
Antibiotic treatment (yes/no)	**43/15**	**17/45**	**3.14×10^{-7}**	**$\chi^2(1)$= 26.16**
Antiviral treatment (yes/no)	**41/17**	**1/61**	**2.23×10^{-15}**	**$\chi^2(1)$= 62.85**
qSOFA (0/1/2)	19/29/10	27/34/1	1.10×10^{-2}	$\chi^2(2) = 9.03$
Neurological complications and confounding variables				
Agitation (yes/no)	**25/33**	**10/52**	**1.20×10^{-3}**	**$\chi^2(1)$= 10.55**
Cerebrovascular event (yes/no)	39/19	36/26	0.30	$\chi^2(1) = 1.08$
Diabetes (yes/no)	15/43	7/55	3.93×10^{-2}	$\chi^2(1) = 4.25$
Hypertension (yes/no)	30/28	41/21	0.11	$\chi^2(1) = 2.57$

Note, the *p* value and effect size are for COVID-19 vs. non-COVID-19 difference. Rows in bold are variables showing significant COVID-19 vs. non-COVID-19 difference (corrected for twelve tests)). Pneumonia value of 1 denotes COVID/interstitial pneumonia, and pneumonia value of 0 denotes other/no pneumonia. **Abbreviations:** GCS, Glasgow Coma Score; qSOFA, quick Sequential Organ Failure.

Among 120 CT images, 54 were scanned with the Somatom Definition Edge, and the remaining 66 were acquired with the Aquilon Prime. The scanner allocation was relatively balanced between COVID-19 and non-COVID-19 groups (p = 0.49 for COVID-19 vs. non-COVID-19). Outcome (dead/discharged), good outcome, mRS at discharge and six months follow-up showed significant COVID-19 vs. non-COVID-19 difference. Given the relatively small sample size and the observation that mRS scores provided more information of outcome, mRS scores at discharge and six months follow-up were selected to further test their associations with GMV loadings of decomposed 15 GMV.

3.2. Summary of COVID-19 characteristics and confounding variables

Table 2 lists the clinical characteristics (symptoms and treatments) of COVID-19 and its neurological complications as well as the confounding factors. Diagnosis of pneumonia, fever, an indicator of a respiratory rate greater than 21, oxygen therapy, antibiotics and antiviral treatments, and agitation presented significant COVID-19 vs. non-COVID-19 difference. COVID-19 patients receiving oxygen therapy had significantly larger BCRSS values (i.e., severe COVID-19 symptom) compared to COVID-19 patients not receiving oxygen therapy (p = 3.28 x10^{-5}). BCRSS values of COVID-19 patients with fever were not different from that of COVID-19 patients without fever (p = 0.42). Due to the relatively small sample size and high prevalence of fever and lack of oxygen in COVID-19 patients, receipt of oxygen therapy and fever status were selected as the most important COVID-19 variables to further test their associations with loadings of decomposed 15 GMV components.

Note that the scanner allocation was significantly related to mRS at

discharge ($p = 2.51 \times 10^{-2}$) and at six months follow-up ($p = 2.73 \times 10^{-2}$), as well as the status of oxygen therapy ($p = 2.47 \times 10^{-2}$) (see details in Supplemental Table S1). Thus, the interaction term between scanner allocation and the clinical variable was considered as an additional predictor while correcting the scanner effect.

3.3. Results from source-based morphometry analysis

The total GMV did not show significant COVID-19 vs. non-COVID-19 difference ($p > 0.5$). Among 15 independent GMV components, no components showed significant COVID-19 vs. non-COVID-19 difference ($p > 0.05$).

Two GMV components were significantly related to clinical measures of COVID-19 after MAFDR at $p < 0.05$ correction of 60 tests (15 GMV components × 4 clinical variables (mRS at discharge, mRS at 6 months follow-up, fever, receipt of oxygen therapy)). As plotted in Fig. 1, GMV component 1 (IC 1, Fig. 1(a)) in superior/medial/middle frontal gyri was significantly and negatively associated with the mRS score at discharge (Fig. 1(b), $p = 1.03 \times 10^{-3}$, $R^2 = 11.55\%$, $t = -3.37$, degree of freedom (DF) = 115, MAFDR corrected $p = 3.50 \times 10^{-2}$) and at 6-month follow-up (Fig. 1(c), $p = 1.71 \times 10^{-3}$, $R^2 = 10.28\%$, $t = -3.21$, DF = 115, MAFDR corrected $p = 2.92 \times 10^{-2}$), showing that the higher the mRS score (higher level of disability) at discharge and at 6-month follow-up phases, the lower the GMV in superior/medial/middle frontal gyri. Moreover, participants received oxygen therapy showed significantly lower GMV in superior/medial/middle frontal gyri compared to individuals not received oxygen therapy after controlling for COVID-19 diagnosis (Fig. 1(d), $p = 3.48 \times 10^{-3}$, $t = -2.98$, DF = 115, MAFDR corrected $p = 2.97 \times 10^{-2}$). When narrowing the sample down to 58 COVID-19 patients, we observed that COVID-19 patients received oxygen therapy presented GMV reduction in superior/medial/middle frontal gyri compared to COVID-19 patients not received oxygen therapy ($p = 1.73 \times 10^{-2}$, $t = -2.46$, DF = 54).

Fig. 2 plots that GMV IC 2 in inferior/middle temporal gyri and fusiform gyrus (Fig. 2(a)) was significantly related to fever status (Fig. 2(b), $p = 2.31 \times 10^{-3}$, $t = -3.12$, DF = 115, MAFDR corrected $p = 2.62 \times 10^{-2}$), where participants with fever had significantly lower GMV compared to individuals without fever. Focusing on 58 COVID-19 patients, we observed that COVID-19 patients with fever presented GMV reduction in inferior/middle temporal gyri and fusiform gyrus compared to COVID-19 patients without fever ($p = 9.44 \times 10^{-3}$, $t = -2.69$, DF = 54). COVID-19 patients showed nonsignificant GMV reduction in GMV IC 1 and IC 2 compared to patients without COVID-19 (IC 1: $p = 0.09$; IC 2: $p = 0.25$). The identified associations were not confounded with cerebrovascular events, hypertension or diabetes (see Supplemental Table S2 for details). Brain regions ($|Z| > 2$, cluster volume > 1 cm^3), the corresponding volume, and peak voxel coordinates of GMV IC 1–2 are listed in Table 3.

Moreover, the associations identified from full samples were held in 58 COVID-19 patients (see Supplemental Table S3 for details). The severity of COVID-19 disease (BCRSS score) marginally and negatively associated with loadings of GMV IC 1 among 58 COVID-19 patients ($p = 0.08$), but not related to that of GMV IC 2 ($p > 0.5$). Among all included 120 participants, patients with COVID/interstitial pneumonia showed GMV reduction in IC 1 compared to patients with other/no pneumonia after controlling for COVID-19 diagnosis ($p = 3.84$ x10^{-2}). GMV reduction was not presented in patients with COVID/interstitial pneumonia for IC 2 ($p > 0.5$).

After controlling the scanner effect on full samples, we observed that associations between IC 1 and mRS scores at both discharge and 6-month follow-up were still significant (discharge: $p = 3.11 \times 10^{-3}$; follow-up: $p = 3.46 \times 10^{-3}$). IC 2 was still significantly related to fever status ($p = 2.76 \times 10^{-3}$). The association between IC 1 and oxygen therapy was held with reduced significance ($p = 1.16 \times 10^{-2}$). The inferences were the same as those without controlling the scanner effect. Most of the identified associations were held in subsamples acquired from the individual scanner (Toshiba or Siemens) (see details results in Supplemental Table S4).

Focusing on 66 individuals with normal CT scans, we observed that the association between IC 1 and receipt of oxygen therapy was still significant ($p = 1.80 \times 10^{-3}$, $t = -3.27$, DF = 61); The association between IC 2 and fever status was held ($p = 0.03$, $t = -2.16$, DF = 61). The remaining associations were marginally significant ($p < 0.1$) and shared similar trends as that from full samples (see Supplemental Table S5 for details).

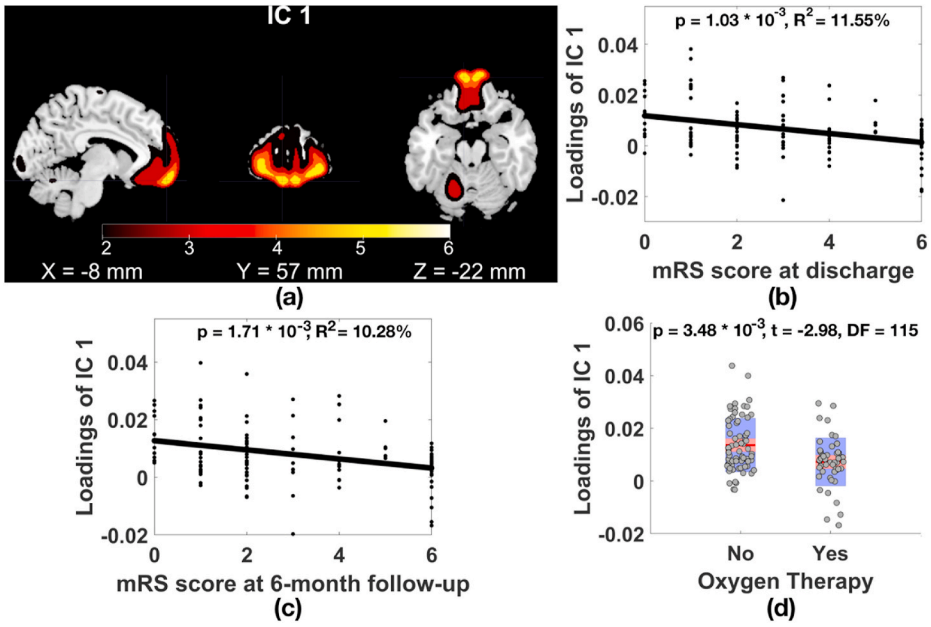

Fig. 1. (a) GMV IC 1 in superior/medial/middle frontal gyri ($|Z|>2$) significantly associated with the mRS score at (b) discharge and (c) 6-month follow-up, and (d) oxygen therapy status. Note, for loadings of GMV IC 1 in Fig. 1(b–d), effects from age, gender, and COVID-19 diagnosis were regressed out.

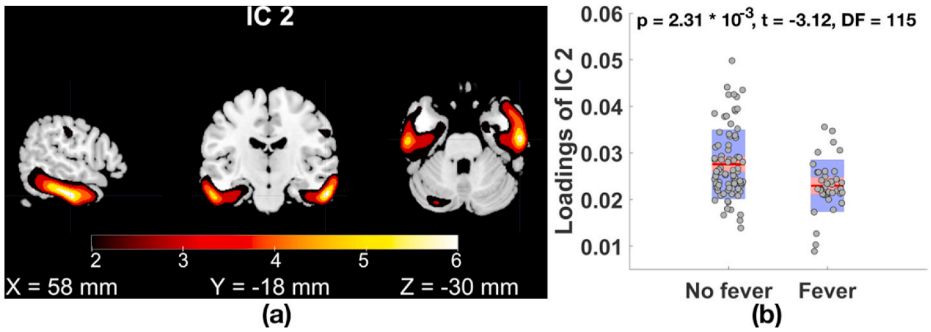

Fig. 2. (a) GMV IC 2 in inferior/middle temporal gyri and fusiform gyrus (|Z|>2) significantly related to (b) fever status (for loadings of GMV IC2, effects from age, gender, and COVID-19 diagnosis were regressed out).

Table 3
Talairach labels, peak voxel coordinates in Talairach space and volume of GMV IC 1–2 (|Z| > 2, cluster volume > 1 cm^3).

GMV IC	Brain regions (Brodmann area)	L/R volume (cm3)	L/R: max Z (x, y, z)
IC 1	Superior Frontal Gyrus (10, 11)	4.8/5.0	4.7 (−9, 57, −19)/4.7 (30, 54, −11)
	Medial Frontal Gyrus (10, 11, 25)	1.8/1.9	4.7 (−10, 58, −16)/4.7 (10, 60, −16)
	Middle Frontal Gyrus (10, 11, 47)	2.3/1.5	4.1 (−31, 53, −3)/4.1 (31, 55, −7)
IC 2	Inferior Temporal Gyrus (20, 21, 37)	3.9/5.4	4.6 (−59, −27, −17)/5.1 (59, −22, −20)
	Fusiform Gyrus (20, 36, 37)	2.0/1.9	4.0 (−56, −32, −19)/5.1 (57, −16, −23)
	Middle Temporal Gyrus (20, 21, 37,38)	1.2/5.1	3.5 (−61, −30, −13)/4.6 (62, −32, −11)

3.4. Results from voxel-based morphometry analysis

Similar to the SBM analysis, no voxels showed significant COVID-19 vs. non-COVID-19 differences after FDR correction for VBM. Given the relatively small sample size and the large number of association tests conducted, no voxels showed significant associations with the mRS score at discharge or 6 months follow-up, presence of oxygen therapy, or fever status after FDR correction. However, the highlighted brain regions (|T|>2, Fig. 3, the positive and negative signs were flipped to be consistent with the spatial map plots of GMV IC 1–2 in Figs. 1(a) and 2(a)) were largely overlapped with the identified GMV ICs 1–2 and shared the same inference with SBM results regarding the mRS score at discharge and 6 months follow-up, oxygen therapy status and fever status.

3.4. mRS prediction results

Based on SVR with LASSO, loadings of frontal and temporal components (CT model) significantly predicted mRS scores at both discharge ($r = 0.50$, $p = 2.04 \times 10^{-3}$, MSE = 4.43) and 6-month follow up ($r = 0.39$, $p = 1.77 \times 10^{-2}$, MSE = 5.19) for the testing set. Adding clinical and demographic variables into the model (CT + clinic model), the mRS prediction accuracy increased for both discharge ($r = 0.67$, $p = 9.10 \times 10^{-6}$, MSE = 3.22) and 6-month follow up ($r = 0.67$, $p = 7.06 \times 10^{-6}$, MSE = 3.27). The prediction accuracies for mRS at discharge from CT model and CT + clinic model, and weights of selected variables from CT + clinic model are plotted in Fig. 4(a) and (b), respectively (results for mRS at follow-up are plotted in Supplemental Fig. S1). Age, loadings of the GMV IC 1 (frontal region), and receipt of oxygen therapy were strong predictors (with large weights) for mRS at discharge and follow-up predictions, where older age, lower GMV in the frontal region and

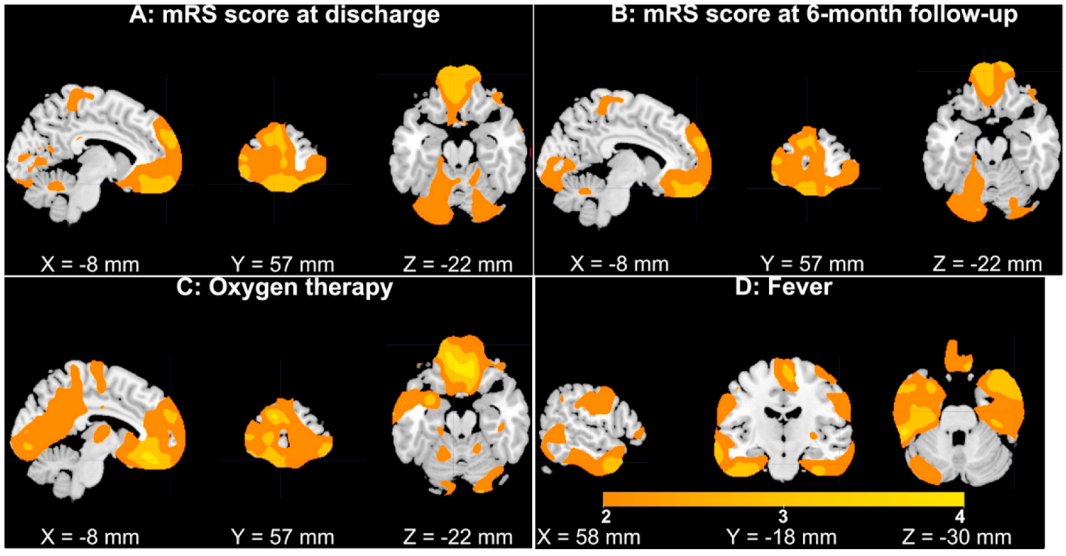

Fig. 3. Results of VBM analysis (|T| > 2). Colors are coded for T values (the positive and negative signs were flipped) of association results. GMV in superior/medial/middle frontal gyri was negatively correlated with the mRS score at discharge (subplot A) and 6 months follow-up (subplot B) and associated with the presence of oxygen therapy (subplot C, participants receiving oxygen therapy had lower GMV compared to individuals not receiving oxygen therapy). Individuals suffering from fever had lower GMV in the inferior/middle temporal gyri and fusiform gyrus compared to individuals without a fever (subplot D). (For interpretation of the references to color in this figure legend, the reader is referred to the Web version of this article.)

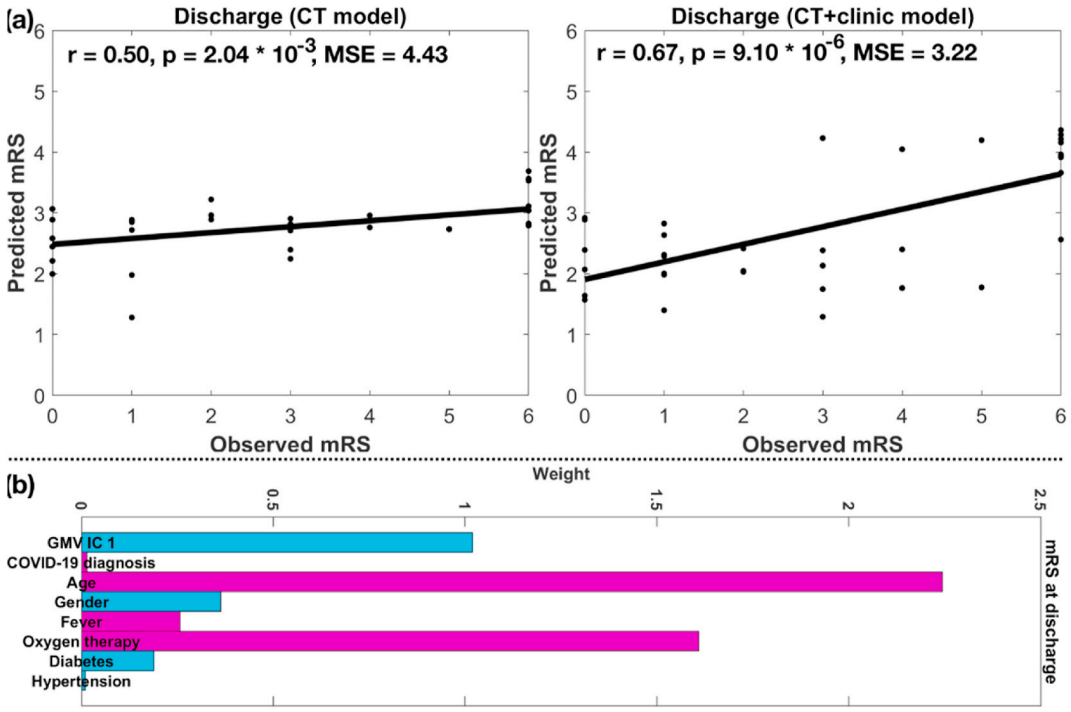

Fig. 4. (a) Prediction accuracies of mRS at discharge based on CT and CT + clinic models, (b) weight of selected variables from CT + clinic model. Note, cyan and magenta colors in (b) denote negative and positive weights, respectively (same for Fig. S1 (b)). (For interpretation of the references to color in this figure legend, the reader is referred to the Web version of this article.)

lack of oxygen were associated with larger mRS score (i.e., higher level of disability).

4. Discussion

This study investigated CT-derived GMV alterations underlying COVID-19 in 120 older adults by using SBM analysis. No brain regions showed a significant difference between adults with COVID-19 and adults without COVID-19. However, lower GMV in superior/medial/middle frontal gyri was related to higher mRS score (i.e., a higher level of disability) at both discharge and 6 months follow-up phases. Patients who received oxygen therapy presented reduced GMV in superior/medial/middle frontal gyri compared to patients who not received oxygen therapy. GMV in inferior/middle temporal gyri and fusiform gyrus was significantly reduced in patients with fever compared to patients without fever. These associations/alterations were still significant after controlling for cerebrovascular diseases, diabetes, and hypertension. SBM results were also consistent with the voxel-wise patterns identified in the VBM results. The reported associations were largely held in subsamples of normal CT images and in full samples with controlling scanner effect, indicating that the identified associations were less likely driven by vascular lesions or scanner difference.

The associated clinical measures are well characterized by COVID-19. COVID-19 patients had higher mRS scores (i.e., a higher level of disability) than individuals without COVID-19 at discharge, even though both groups shared similar baseline mRS scores (Pilotto et al., 2020). Fever has been recognized as the most common symptom of hospitalized COVID-19 patients (Benussi et al., 2020; Ng et al., 2020; Qiu et al., 2020; Wang et al., 2020). Oxygen therapy has been widely taken for COVID-19 patients (Barrett et al., 2020; Hassan et al., 2020; Kayem et al., 2020; Liu et al., 2020; Paganini et al., 2020).

The result that patients who received oxygen therapy presented reduced GMV in frontal regions can be supported by the observations that individuals who were lack of oxygen supply to the brain demonstrated regional GMV reduction (Zhang et al., 2013; Harch and Fogarty, 2017). Patients with chronic obstructive pulmonary disease that can cause reduced oxygen supply to the brain have shown GMV reduction in widespread regions, including the frontal cortex, the cingulate cortex, and other subcortical regions (Zhang et al., 2013). A two-year-old girl who suffered from water drowning demonstrated GMV atrophy in temporal, parietal, and cerebellar lobes, and the GMV atrophy was dramatically improved after receiving oxygen therapy (Harch and Fogarty 2017).

Brain structure/function/metabolism/activity of frontal and temporal lobes are increasingly reported as being affected by COVID-19. In T2-weighted MRI studies, COVID-19 patients presented white matter hyperintensity in frontal cortical region/right frontal lobe/right prefrontal cortex with (Kaya et al., 2020) or without oxygen therapy (Anzalone et al., 2020; Koh et al., 2020; Le Guennec, Devianne et al., 2020; Umapathi et al., 2020). Recovered COVID-19 patients manifested lower mean diffusivity and axial diffusivity in the right superior frontal-occipital fasciculus (Lu et al., 2020). In studies of CT head images, COVID-19 patients showed hypodensity in right/posterior frontal gyri in white matter (Princiotta Cariddi, Tabaee Damavandi et al. 2020) or white and gray matter (Goel et al., 2020). In EEG studies, COVID-19 patients demonstrated slow delta waves with diffuse projection but greater amplitude in frontal regions (Vellieux et al., 2020). In 18F-FDG-PET studies, COVID-19 patients presented hypometabolism in widespread cerebral regions, including the frontal cortex, insular and subcortical regions, which still existed at six months post COVID-19 diagnosis (Kas et al., 2021). A series of COVID-19 patients presented hypometabolism in prefrontal and orbitofrontal cortexes (Delorme et al., 2020; Karimi-Galougahi et al., 2020) and hypermetabolism in cerebellar vermis (Delorme et al., 2020). Particularly, frontal hypometabolism was related to new-onset cognitive disturbance (Delorme et al., 2020). Another study reported that GM cortical thickness of orbitofrontal regions was negatively associated with the Beck Anxiety Inventory score of COVID-19 patients (Crunfli et al., 2020). Moreover, COVID-19 patients with fever demonstrated white matter hyperintensities in the temporal lobe (Anand et al., 2020a,b) and bilateral medial temporal lobes (Poyiadji et al., 2020), and hypometabolism in bilateral prefrontal and left-sided parietal-temporal lobes (Delorme et al., 2020). COVID-19

patients also presented symmetric bilateral hypodensity in the temporal region in CT head images (Princiotta Cariddi, Tabaee Damavandi et al. 2020) and EEG dysfunction (occasional independent sharp waves) in the right posterior temporal region (Anand et al., 2020a). Bilateral fronto-temporal hypoperfusion was also recognized in COVID-19 patients (Helms et al., 2020). More importantly, a different population of COVID-19 patients, i.e., patients with long COVID-19 (enduring functional impairments after apparent recovery from COVID-19), presented hypometabolism in focal brain regions including frontal and right temporal lobes, brainstem and cerebellum, where metabolism values in frontal and temporal lobes correctly classified patients with long COVID-19 and healthy controls and were associated with enduring pain/high blood pressure/insomnia (Guedj et al., 2021). These findings together with our results indicate that frontal and temporal abnormalities are presented in acute COVID-19 patients, and these abnormalities are likely persistent even after recovery from COVID-19.

GMV in the frontal-temporal network was not related to the severity of COVID-19 symptoms (BCRSS score) and did not show a significant difference between COVID-19 patients with diabetes and COVID-19 patients without diabetes ($p > 0.05$), although more diabetes was observed in COVID-19 patients compared to participants without COVID-19 ($p = 3.93 \times 10^{-2}$). However, GMV in a frontal-temporal network was reduced in patients receiving oxygen therapy or with fever compared to those not receiving oxygen therapy or without fever. Moreover, COVID-19 patients receiving oxygen therapy or with fever presented GMV reduction ($p < 0.05$, Supplemental Table S3) in the identified frontal-temporal network compared to COVID-19 patients not receiving oxygen therapy or without fever. The previous study has reported hypoxic injuries in the cerebrum and cerebellum with loss of neurons in the cerebral cortex, hippocampus, and cerebellar Purkinje cell layer in 18 patients who died from COVID-19, and no encephalitis or other specific brain changes were observed directly caused by the virus for these 18 patients (Solomon et al., 2020). These findings, together with our results, indicate that COVID-19 may not affect the brain directly. Instead, it may affect the frontal-temporal network in a secondary manner through fever or lack of oxygen (hypoxia).

The absence of findings of GMV networks presenting COVID-19 vs. non-COVID-19 difference may be caused by two reasons: (1) This study analyzed CT images, which were widely used for clinical diagnosis but may not well capture (subtle) GMV alterations introduced by COVID-19. (2) brain alterations caused by COVID-19 may not have occurred yet or were at the early stage of progression at the time CT scans were taken. To date, MRI scans employed in two published studies that detected GM alterations related to COVID-19 were taken three months (Lu et al., 2020) or with a median of 54 days (Crunfli et al., 2020) after a COVID-19 diagnosis. CT scans of COVID-19 patients included in this study were taken 1–17 (4.5 ± 3.34) days following COVID-19 diagnosis.

The current study should be considered in light of strengths and limitations. This study employed SBM, a multivariate version of VBM, to decompose GMV data derived from CT scans into independent sources, and further statistical inferences were conducted at the source level, which reduced the number of tests and boosted statistical power. SBM-identified brain regions related to clinical measures of COVID-19 were consistent with those from VBM. The limitations may include (i) the findings presented in this study may not be generalizable to COVID-19 patients without brain complications, since this study mainly included acute COVID-19 patients that more likely had neurological complications; (ii) this study may fail to detect some COVID-19-related focal brain alterations (for example, brainstem and cerebellum alterations (Guedj et al., 2021)) since CT imaging may not evaluate these regions well; (iii) the absence of CT images of healthy controls may hinder identifications of brain regions potentially discriminating COVID-19 patients from healthy controls; (iv) collecting imaging data prior to COVID-19 is challenging since we cannot predict who will contract the virus. Thus, we cannot rule out the possibility that fever and lack of oxygen existed prior to COVID-19 onsite or definitively link the identified imaging markers to fever/lack of oxygen introduced by COVID-19; (v) as the sample size of this study is relatively small, the generalizability of the findings awaits future validation.

5. Conclusions

This study leveraged a multivariate blind source separation method, SBM, to identify CT-derived GMV alterations underlying COVID-19 in 120 older adults. Results showed that GMV in a frontal-temporal network was reduced in patients receiving oxygen therapy or with fever compared to those not receiving oxygen therapy or without fever. Moreover, patients with higher mRS score (higher level of disability) had lower GMV in superior, medial, and middle frontal gyri at both discharge and at six months follow-up even when controlling for cerebrovascular diseases, indicating that the frontal networks could represent a core/hub region for the brain involvement in COVID-19, beyond the presence of specific (focal) damage related to clinical manifestations (i.e., stroke, ICH, encephalitis) of COVID-19. GMV in the frontal region was reduced in patients with agitation compared to patients without agitation, implying that alterations in the frontal region likely underlie the mood disturbance introduced by COVID-19. Importantly, GMV alterations in the identified frontal-temporal network can predict individual disability levels (i.e., mRS) at both discharge and 6 months follow-up for the hold-out testing samples, implying that the frontal-temporal network can be potentially employed as a biomarker for prognosis and evaluation of treatment of COVID-19.

Author contributions

K. D., V. C., and E. P. designed the study. E. P. and A. P. acquired the data and consulted on the interpretation. J. B. helped with the preprocessing. K. D. analyzed the data and wrote the manuscript. V. C., E. P. and A. P. assisted with writing. The remaining authors contributed to participant recruitment and data collection. All authors critically reviewed the content and approved the final version for publication.

Declaration of competing interest

Andrea Pilotto is consultant and served on the scientific advisory board of Z-cube (Technology Division of Zambon Pharma), received speaker honoraria from Abbvie, Biomarin and Zambon Pharmaceuticals.

Alessandro Padovani received grant support from Ministry of Health (MINSAL) and Ministry of Education, Research and University (MIUR), from CARIPLO Foundation; personal compensation as a consultant/scientific advisory board member for Avanir, Lundbeck, Eli-Lilly, Neuraxpharma, Biogen, GE Health.

The other authors report no conflict of interest.

Acknowledgments

This study was supported by The National Institutes of Health and The National Institute on Aging through the grant 3RF1AG063153-01A1S1. The authors thank all participants involved in this project.

Appendix A. Supplementary data

Supplementary data to this article can be found online at https://doi.org/10.1016/j.ynstr.2021.100326.

References

Agyeman, A.A., Chin, K.L., Landersdorfer, C.B., Liew, D., Ofori-Asenso, R., 2020. Smell and taste dysfunction in patients with COVID-19: a systematic review and meta-analysis. Mayo Clin. Proc. 95 (8), 1621–1631.

Anand, P., Al-Faraj, A., Sader, E., Dashkoff, J., Abdennadher, M., Murugesan, R., Cervantes-Arslanian, A.M., Daneshmand, A., 2020a. Seizure as the presenting symptom of COVID-19: a retrospective case series. Epilepsy Behav. 112, 107335.

Anand, P., Lau, K.H.V., Chung, D.Y., Virmani, D., Cervantes-Arslanian, A.M., Mian, A.Z., Takahashi, C.E., 2020b. Posterior reversible encephalopathy syndrome in patients with coronavirus disease 2019: two cases and A review of the literature. J. Stroke Cerebrovasc. Dis. 29 (11), 105212.
Anzalone, N., Castellano, A., Scotti, R., Scandroglio, A.M., Filippi, M., Ciceri, F., Tresoldi, M., Falini, A., 2020. Multifocal laminar cortical brain lesions: a consistent MRI finding in neuro-COVID-19 patients. J. Neurol. 267 (10), 2806–2809.
Asadi-Pooya, A.A., 2020. Seizures associated with coronavirus infections. Seizure 79, 49–52.
Asadi-Pooya, A.A., Simani, L., 2020. Central nervous system manifestations of COVID-19: a systematic review. J. Neurol. Sci. 413, 116832.
Barrett, R., Catangui, E., Scott, R., 2020. Acute oxygen therapy: a cross-sectional study of prescribing practices at an English hospital immediately before COVID-19 pandemic. Expet Rev. Respir. Med.
Bell, A.J., Sejnowski, T.J., 1995. An information maximization approach to blind separation and blind deconvolution. Neural Comput. 7 (6), 1129–1159.
Benussi, A., Pilotto, A., Premi, E., Libri, I., Giunta, M., Agosti, C., Alberici, A., Baldelli, E., Benini, M., Bonacina, S., Brambilla, L., Caratozzolo, S., Cortinovis, M., Costa, A., Cotti Piccinelli, S., Cottini, E., Cristillo, V., Delrio, I., Filosto, M., Gamba, M., Gazzina, S., Gilberti, N., Gipponi, S., Imarisio, A., Invernizzi, P., Leggio, U., Leonardi, M., Liberini, P., Locatelli, M., Masciocchi, S., Poli, L., Rao, R., Risi, B., Rozzini, L., Scalvini, A., Schiano di Cola, F., Spezi, R., Vergani, V., Volonghi, I., Zoppi, N., Borroni, B., Magoni, M., Pezzini, A., Padovani, A., 2020. Clinical characteristics and outcomes of inpatients with neurologic disease and COVID-19 in Brescia, Lombardy, Italy. Neurology 95 (7), e910–e920.
Benussi, A., Premi, E., Pilotto, A., Libri, I., Pezzini, A., Paolillo, C., Borroni, B., Magoni, M., Padovani, A., 2021. Effects of COVID-19 outbreak on stroke admissions in Brescia, Lombardy, Italy. Eur. J. Neurol. 28 (1), e4–e5.
Brudfors, M., 2020. Generative Models for Preprocessing of Hospital Brain Scans. UCL (University College London.
Brudfors, M., Balbastre, Y., Flandin, G., Nachev, P., Ashburner, J., 2020. Flexible Bayesian Modelling for Nonlinear Image Registration arXiv preprint arXiv: 2006.02338.
Calhoun, V.D., Adali, T., Pearlson, G.D., Pekar, J.J., 2001. A method for making group inferences from functional MRI data using independent component analysis. Hum. Brain Mapp. 14 (3), 140–151.
Carrillo-Larco, R.M., Altez-Fernandez, C., 2020. Anosmia and dysgeusia in COVID-19: a systematic review. Wellcome Open Res. 5, 94.
Chen, J., Liu, J., Calhoun, V.D., Arias-Vasquez, A., Zwiers, M.P., Gupta, C.N., Franke, B., Turner, J.A., 2014. Exploration of scanning effects in multi-site structural MRI studies. J. Neurosci. Methods 230, 37–50.
Choi, Y., Lee, M.K., 2020. Neuroimaging findings of brain MRI and CT in patients with COVID-19: a systematic review and meta-analysis. Eur. J. Radiol. 133, 109393.
Crunfli, F., Carregari, V.C., Veras, F.P., Vendramini, P.H., Fragnani Valença, A.G., Leão Marcelo Antunes, A.S., Brandão-Teles, C., da Silva Zuccoli, G., Reis-de-Oliveira, G., Silva-Costa, L.C., Saia-Cereda, V.M., Codo, A.C., Parise, P.L., Toledo-Teixeira, D.A., de Souza, G.F., Muraro, S.P., Silva Melo, B.M., Almeida, G.M., Silva Firmino, E.M., Paiva, I.M., Souza Silva, B.M., Ludwig, R.G., Ruiz, G.P., Knittel, T.L., Gastão Davanzo, G., Gerhardt, J.A., Rodrigues, P.B., Forato, J., Amorim, M.R., Silva, N.B., Martini, M.C., Benatti, M.N., Batah, S., Siyuan, L., João, R.B., Silva, L.S., Nogueira, M.H., Aventurato, Í.K., de Brito, M.R., Machado Alvim, M.K., da Silva Júnior, J.R., Damião, L.L., de Paula Castilho Stefano, M.E., Pereira de Sousa, I.M., da Rocha, E.D., Gonçalves, S.M., Lopes da Silva, L.H., Bettini, V., de Campos, B.M., Ludwig, G., Mendes Viana, R.M., Martins, R., Vieira, A.S., Alves-Filho, J.C., Arruda, E., Sebollela, A.S., Cendes, F., Cunha, F.Q., Damásio, A., Ramirez Vinolo, M. A., Munhoz, C.D., Rehen, S.K., Mauad, T., Duarte-Neto, A.N., Ferraz da Silva, L.F., Dolhnikoff, M., Saldiva, P., Fabro, A.T., Farias, A.S., Moraes-Vieira, P.M.M., Proença Módena, J.L., Yasuda, C.L., Mori, M.A., Cunha, T.M., Martins-de-Souza, D., 2020. SARS-CoV-2 infects brain astrocytes of COVID-19 patients and impairs neuronal viability. medRxiv. https://doi.org/10.1101/2020.10.09.20207464.
Delorme, C., Paccoud, O., Kas, A., Hesters, A., Bombois, S., Shambrook, P., Boullet, A., Doukhi, D., Le Guennec, L., Godefroy, N., Maatoug, R., Fossati, P., Millet, B., Navarro, V., Bruneteau, G., Demeret, S., Pourcher, V., g. CoCo-Neurosciences study, C. S. P. s. group, 2020. COVID-19-related encephalopathy: a case series with brain FDG-positron-emission tomography/computed tomography findings. Eur. J. Neurol. 27 (12), 2651–2657.
Egbert, A.R., Cankurtaran, S., Karpiak, S., 2020. Brain abnormalities in COVID-19 acute/subacute phase: a rapid systematic review. Brain Behav. Immun. 89, 543–554.
Espinosa, P.S., Rizvi, Z., Sharma, P., Hindi, F., Filatov, A., 2020. Neurological complications of coronavirus disease (COVID-19): encephalopathy, MRI brain and cerebrospinal fluid findings: case 2. Cureus 12 (5) e7930.
Filatov, A., Sharma, P., Hindi, F., Espinosa, P.S., 2020. Neurological complications of coronavirus disease (COVID-19): encephalopathy. Cureus 12 (3) e7352.
Frontera, J.A., Sabadia, S., Lalchan, R., Fang, T., Flusty, B., Millar-Vernetti, P., Snyder, T., Berger, S., Yang, D., Granger, A., Morgan, N., Patel, P., Gutman, J., Melmed, K., Agarwal, S., Bokhari, M., Andino, A., Valdes, E., Omari, M., Kvernland, A., Lillemoe, K., Chou, S.H., McNett, M., Helbok, R., Mainali, S., Fink, E.L., Robertson, C., Schober, M., Suarez, J.I., Ziai, W., Menon, D., Friedman, D., Friedman, D., Holmes, M., Huang, J., Thawani, S., Howard, J., Abou-Fayssal, N., Krieger, P., Lewis, A., Lord, A.S., Zhou, T., Kahn, D.E., Czeisler, B.M., Torres, J., Yaghi, S., Ishida, K., Scher, E., de Havenon, A., Placantonakis, D., Liu, M., Wisniewski, T., Troxel, A.B., Balcer, L., Galetta, S., 2020. A prospective study of neurologic disorders in hospitalized COVID-19 patients in New York city. Neurology.
Goel, V., Goyal, B., Mathur, A., Chand, G., Marwaha, V., Dhar, A., 2020. An institutional based study on imaging conundrum of newly diagnosed coronavirus disease 2019 (COVID-19)–A retrospective analysis in India population. Int J Cur Res Rev| 12 (19), 5.
Guedj, E., Campion, J.Y., Dudouet, P., Kaphan, E., Bregeon, F., Tissot-Dupont, H., Guis, S., Barthelemy, F., Habert, P., Ceccaldi, M., Million, M., Raoult, D., Cammilleri, S., Eldin, C., 2021. (18)F-FDG brain PET hypometabolism in patients with long COVID. Eur. J. Nucl. Med. Mol. Imag.
Harch, P.G., Fogarty, E.F., 2017. Subacute normobaric oxygen and hyperbaric oxygen therapy in drowning, reversal of brain volume loss: a case report. Med. Gas Res. 7 (2), 144–149.
Hassan, S.A., Sheikh, F.N., Jamal, S., Ezeh, J.K., Akhtar, A., 2020. Coronavirus (COVID-19): a review of clinical features, diagnosis, and treatment. Cureus 12 (3) e7355.
Helms, J., Kremer, S., Merdji, H., Clere-Jehl, R., Schenck, M., Kummerlen, C., Collange, O., Boulay, C., Fafi-Kremer, S., Ohana, M., Anheim, M., Meziani, F., 2020. Neurologic features in severe SARS-CoV-2 infection. N. Engl. J. Med. 382 (23), 2268–2270.
Himberg, J., Hyvarinen, A., Esposito, F., 2004. Validating the independent components of neuroimaging time series via clustering and visualization. Neuroimage 22 (3), 1214–1222.
Kandemirli, S.G., Dogan, L., Sarikaya, Z.T., Kara, S., Akinci, C., Kaya, D., Kaya, Y., Yildirim, D., Tuzuner, F., Yildirim, M.S., Ozluk, E., Gucyetmez, B., Karaarslan, E., Koyluoglu, I., Demirel Kaya, H.S., Mammadov, O., Kisa Ozdemir, I., Afsar, N., Citci Yalcinkaya, B., Rasimoglu, S., Guduk, D.E., Kedir Jima, A., Ilksoz, A., Ersoz, V., Yonca Eren, M., Celtik, N., Arslan, S., Korkmazer, B., Dincer, S.S., Gulek, E., Dikmen, I., Yazici, M., Unsal, S., Ljama, T., Demirel, I., Ayyildiz, A., Kesimci, I., Bolsoy Deveci, S., Tutuncu, M., Kizilkilic, O., Telci, L., Zengin, R., Dincer, A., Akinci, I.O., Kocer, N., 2020. Brain MRI findings in patients in the intensive care unit with COVID-19 infection. Radiology 297 (1), E232–E235.
Karimi-Galougahi, M., Yousefi-Koma, A., Bakhshayeshkaram, M., Raad, N., Haseli, S., 2020. (18)FDG PET/CT scan reveals hypoactive orbitofrontal cortex in anosmia of COVID-19. Acad. Radiol. 27 (7), 1042–1043.
Kas, A., Soret, M., Pyatigoskaya, N., Habert, M.O., Hesters, A., Le Guennec, L., Paccoud, O., Bombois, S., Delorme, C., g. on the behalf of CoCo-Neurosciences study, C. S. P. s. group, 2021. The cerebral network of COVID-19-related encephalopathy: a longitudinal voxel-based 18F-FDG-PET study. Eur. J. Nucl. Med. Mol. Imag.
Kaya, Y., Kara, S., Akinci, C., Kocaman, A.S., 2020. Transient cortical blindness in COVID-19 pneumonia; a PRES-like syndrome: case report. J. Neurol. Sci. 413, 116858.
Kayem, G., Lecarpentier, E., Deruelle, P., Bretelle, F., Azria, E., Blanc, J., Bohec, C., Bornes, M., Ceccaldi, P.F., Chalet, Y., Chauleur, C., Cordier, A.G., Desbriere, R., Doret, M., Dreyfus, M., Driessen, M., Fermaut, M., Gallot, D., Garabedian, C., Huissoud, C., Luton, D., Morel, O., Perrotin, F., Picone, O., Rozenberg, P., Sentilhes, L., Sroussi, J., Vayssiere, C., Verspyck, E., Vivanti, A.J., Winer, N., Alessandrini, V., Schmitz, T., 2020. A snapshot of the Covid-19 pandemic among pregnant women in France. J. Gynecol. Obstetrics Hum. Reprod. 49 (7).
Koh, J.S., De Silva, D.A., Quek, A.M.L., Chiew, H.J., Tu, T.M., Seet, C.Y.H., Hoe, R.H.M., Saini, M., Hui, A.C., Angon, J., Ker, J.R., Yong, M.H., Goh, Y., Yu, W.Y., Lim, T.C.C., Tan, B.Y.Q., Ng, K.W.P., Yeo, L.L.L., Pang, Y.Z., Prakash, K.M., Ahmad, A., Thomas, T., Lye, D.C.B., Tan, K., Umapathi, T., 2020. Neurology of COVID-19 in Singapore. J. Neurol. Sci. 418, 117118.
Kooraki, S., Hosseiny, M., Myers, L., Gholamrezanezhad, A., 2020. Coronavirus (COVID-19) outbreak: what the department of radiology should know. J. Am. Coll. Radiol. 17 (4), 447–451.
Kremer, S., Lersy, F., de Seze, J., Ferre, J.C., Maamar, A., Carsin-Nicol, B., Collange, O., Bonneville, F., Adam, G., Martin-Blondel, G., Rafiq, M., Geeraerts, T., Delamarre, L., Grand, S., Krainik, A., Group, S.-C., 2020. Brain MRI findings in severe COVID-19: a retrospective observational study. Radiology 297 (2), E242–E251.
Kumari, P., Rothan, H.A., Natekar, J.P., Stone, S., Pathak, H., Strate, P.G., Arora, K., Brinton, M.A., Kumar, M., 2021. Neuroinvasion and encephalitis following intranasal inoculation of SARS-CoV-2 in K18-hACE2 mice. Viruses 13 (1).
Le Guennec, L., Devianne, J., Jalin, L., Cao, A., Galanaud, D., Navarro, V., Boutolleau, D., Rohaut, B., Weiss, N., Demeret, S., 2020. Orbitofrontal involvement in a neuroCOVID-19 patient. Epilepsia 61 (8), e90–e94.
Li, Y.O., Adali, T., Calhoun, V.D., 2007. Estimating the number of independent components for functional magnetic resonance imaging data. Hum. Brain Mapp. 28 (11), 1251–1266.
Liu, K., Chen, Y., Lin, R., Han, K., 2020. Clinical features of COVID-19 in elderly patients: a comparison with young and middle-aged patients. J. Infect. 80 (6), e14–e18.
Lovell, N., Maddocks, M., Etkind, S.N., Taylor, K., Carey, I., Vora, V., Marsh, L., Higginson, I.J., Prentice, W., Edmonds, P., Sleeman, K.E., 2020. Characteristics, symptom management, and outcomes of 101 patients with COVID-19 referred for hospital palliative care. J. Pain Symptom Manag. 60 (1), E77–E81.
Lu, Y., Li, X., Geng, D., Mei, N., Wu, P.Y., Huang, C.C., Jia, T., Zhao, Y., Wang, D., Xiao, A., Yin, B., 2020. Cerebral micro-structural changes in COVID-19 patients - an MRI-based 3-month follow-up study. EClinicalMedicine 25, 100484.
Mao, L., Jin, H., Wang, M., Hu, Y., Chen, S., He, Q., Chang, J., Hong, C., Zhou, Y., Wang, D., Miao, X., Li, Y., Hu, B., 2020. Neurologic manifestations of hospitalized patients with coronavirus disease 2019 in wuhan, China. JAMA Neurol. 77 (6), 683–690.
Moriguchi, T., Harii, N., Goto, J., Harada, D., Sugawara, H., Takamino, J., Ueno, M., Sakata, H., Kondo, K., Myose, N., Nakao, A., Takeda, M., Haro, H., Inoue, O., Suzuki-Inoue, K., Kubokawa, K., Ogihara, S., Sasaki, T., Kinouchi, H., Kojin, H., Ito, M., Onishi, H., Shimizu, T., Sasaki, Y., Enomoto, N., Ishihara, H., Furuya, S., Yamamoto, T., Shimada, S., 2020. A first case of meningitis/encephalitis associated with SARS-Coronavirus-2. Int. J. Infect. Dis. 94, 55–58.
Moro, E., Priori, A., Beghi, E., Helbok, R., Campiglio, L., Bassetti, C.L., Bianchi, E., Maia, L.F., Ozturk, S., Cavallieri, F., Zedde, M., Sellner, J., Bereczki, D., Rakusa, M.,

Di Liberto, G., Sauerbier, A., Pisani, A., Macerollo, A., Soffietti, R., Taba, P., Crean, M., Twardzik, A., Oreja-Guevara, C., Bodini, B., Jenkins, T.M., von Oertzen, T. J., EAN core COVID-19 Task Force, 2020. The international European Academy of Neurology survey on neurological symptoms in patients with COVID-19 infection. Eur. J. Neurol. 27 (9), 1727–1737.

Ng, D.H.L., Choy, C.Y., Chan, Y.H., Young, B.E., Fong, S.W., Ng, L.F.P., Renia, L., Lye, D. C., Chia, P.Y., National Centre for Infectious Diseases, C.-O.R.T., 2020. Fever patterns, cytokine profiles, and outcomes in COVID-19. Open Forum Infect. Dis. 7 (9), ofaa375.

Padovani, A., 2020. Special report COVID-19: neurologists adapt in northern Italy. https://www.eanpages.org/2020/04/01/special-report-covid-19-neurologists-adapt-in-northern-italy/.

Paganini, M., Bosco, G., Perozzo, F.A.G., Kohlscheen, E., Sonda, R., Bassetto, F., Garetto, G., Camporesi, E.M., Thom, S.R., 2020. The role of hyperbaric oxygen treatment for COVID-19: a review. Adv. Exp. Med. Biol.

Paniz-Mondolfi, A., Bryce, C., Grimes, Z., Gordon, R.E., Reidy, J., Lednicky, J., Sordillo, E.M., Fowkes, M., 2020. Central nervous system involvement by severe acute respiratory syndrome coronavirus-2 (SARS-CoV-2). J. Med. Virol. 92 (7), 699–702.

Penny, W.D., Friston, K.J., Ashburner, J.T., Kiebel, S.J., Nichols, T.E., 2011. Statistical Parametric Mapping: the Analysis of Functional Brain Images. Elsevier.

Pezzini, A., Padovani, A., 2020. Lifting the mask on neurological manifestations of COVID-19. Nat. Rev. Neurol. 16 (11), 636–644.

Pilotto, A., Benussi, A., Libri, I., Masciocchi, S., Poli, L., Premi, E., Alberici, A., Baldelli, E., Bonacina, S., Brambilla, L., Benini, M., Caratozzolo, S., Cortinovis, M., Costa, A., Cotti Piccinelli, S., Cottini, E., Cristillo, V., Delrio, I., Filosto, M., Gamba, M., Gazzina, S., Gilberti, N., Gipponi, S., Giunta, M., Imarisio, A., Liberini, P., Locatelli, M., Schiano, F., Rao, R., Risi, B., Rozzini, L., Scalvini, A., Vergani, V., Volonghi, I., Zoppi, N., Borroni, B., Magoni, M., Leonardi, M., Zanusso, G., Ferrari, S., Mariotto, S., Pezzini, A., Gasparotti, R., Paolillo, C., Padovani, A., 2020. COVID-19 impact on consecutive neurological patients admitted to the emergency department. J. Neurol. Neurosurg. Psychiatry.

Pilotto, A., Masciocchi, S., Volonghi, I., Crabbio, M., Magni, E., De Giuli, V., Caprioli, F., Rifino, N., Sessa, M., Gennuso, M., Cotelli, M.S., Turla, M., Balducci, U., Mariotto, S., Ferrari, S., Ciccone, A., Fiacco, F., Imarisio, A., Risi, B., Benussi, A., Premi, E., Foca, E., Caccuri, F., Leonardi, M., Gasparotti, R., Castelli, F., Zanusso, G., Pezzini, A., Padovani, A., S. A.-C.-r. e. S. Group, 2021. Clinical presentation and outcomes of severe acute respiratory syndrome coronavirus 2-related encephalitis: the ENCOVID multicenter study. J. Infect. Dis. 223 (1), 28–37.

Piva, S., Filippini, M., Turla, F., Cattaneo, S., Margola, A., De Fulviis, S., Nardiello, I., Beretta, A., Ferrari, L., Trotta, R., Erbici, G., Foca, E., Castelli, F., Rasulo, F., Lanspa, M.J., Latronico, N., 2020. Clinical presentation and initial management critically ill patients with severe acute respiratory syndrome coronavirus 2 (SARS-CoV-2) infection in Brescia, Italy. J. Crit. Care 58, 29–33.

Poyiadji, N., Shahin, G., Noujaim, D., Stone, M., Patel, S., Griffith, B., 2020. COVID-19-associated acute hemorrhagic necrotizing encephalopathy: imaging features. Radiology 296 (2), E119–E120.

Princiotta Cariddi, L., Tabaee Damavandi, P., Carimati, F., Banfi, P., Clemenzi, A., Marelli, M., Giorgianni, A., Vinacci, G., Mauri, M., Versino, M., 2020. Reversible encephalopathy syndrome (PRES) in a COVID-19 patient. J. Neurol. 267 (11), 3157–3160.

Puelles, V.G., Lutgehetmann, M., Lindenmeyer, M.T., Sperhake, J.P., Wong, M.N., Allweiss, L., Chilla, S., Heinemann, A., Wanner, N., Liu, S., Braun, F., Lu, S., Pfefferle, S., Schroder, A.S., Edler, C., Gross, O., Glatzel, M., Wichmann, D., Wiech, T., Kluge, S., Pueschel, K., Aepfelbacher, M., Huber, T.B., 2020. Multiorgan and renal tropism of SARS-CoV-2. N. Engl. J. Med. 383 (6), 590–592.

Qiu, H., Wu, J., Hong, L., Luo, Y., Song, Q., Chen, D., 2020. Clinical and epidemiological features of 36 children with coronavirus disease 2019 (COVID-19) in Zhejiang, China: an observational cohort study. Lancet Infect. Dis. 20 (6), 689–696.

Rissanen, J., 1978. Paper: modeling by shortest data description. Automatica 14 (5), 465–471.

Rissanen, J., 1983. A universal prior for integers and estimation by minimum description length. Ann. Stat. 416–431.

Salomon, T., Cohen, A., Ben-Zvi, G., Gera, R., Oren, S., Roll, D., Rozic, G., Saliy, A., Tik, N., Tsarfati, G., Tavor, I., Schonberg, T., Assaf, Y., 2020. Brain volumetric changes in the general population following the COVID-19 outbreak and lockdown. https://doi.org/10.1101/2020.09.08.285007 bioRxiv.

Sohal, S., Mansur, M., 2020. COVID-19 presenting with seizures. IDCases, 20. e00782.

Solomon, I.H., Normandin, E., Bhattacharyya, S., Mukerji, S.S., Keller, K., Ali, A.S., Adams, G., Hornick, J.L., Padera Jr., R.F., Sabeti, P., 2020. Neuropathological features of covid-19. N. Engl. J. Med. 383 (10), 989–992.

Storey, J.D., Tibshirani, R., 2003. Statistical significance for genomewide studies. Proc. Natl. Acad. Sci. U. S. A. 100 (16), 9440–9445.

Tian, S., Hu, N., Lou, J., Chen, K., Kang, X., Xiang, Z., Chen, H., Wang, D., Liu, N., Liu, D., Chen, G., Zhang, Y., Li, D., Li, J., Lian, H., Niu, S., Zhang, L., Zhang, J., 2020. Characteristics of COVID-19 infection in Beijing. J. Infect. 80 (4), 401–406.

Umapathi, T., Quek, W.M.J., Yen, J.M., Khin, H.S.W., Mah, Y.Y., Chan, C.Y.J., Ling, L.M., Yu, W.Y., 2020. Encephalopathy in COVID-19 patients; viral, parainfectious, or both? eNeurologicalSci. 21, 100275.

Vellieux, G., Rouvel-Tallec, A., Jaquet, P., Grinea, A., Sonneville, R., d'Ortho, M.-P., 2020. COVID-19 associated encephalopathy: is there a specific EEG pattern? Clin. Neurophysiol.

Wang, D., Hu, B., Hu, C., Zhu, F., Liu, X., Zhang, J., Wang, B., Xiang, H., Cheng, Z., Xiong, Y., 2020. Clinical characteristics of 138 hospitalized patients with 2019 novel coronavirus–infected pneumonia in Wuhan, China. Jama 323 (11), 1061–1069.

Weisscher, N., Vermeulen, M., Roos, Y.B., De Haan, R.J., 2008. What should be defined as good outcome in stroke trials; a modified Rankin score of 0-1 or 0-2? J. Neurol. 255 (6), 867–874.

Wilson, J.T., Hareendran, A., Grant, M., Baird, T., Schulz, U.G., Muir, K.W., Bone, I., 2002. Improving the assessment of outcomes in stroke: use of a structured interview to assign grades on the modified Rankin Scale. Stroke 33 (9), 2243–2246.

Wong, D.K.C., Gendeh, H.S., Thong, H.K., Lum, S.G., Gendeh, B.S., Saim, A., Salina, H., 2020. A review of smell and taste dysfunction in COVID-19 patients. Med. J. Malaysia 75 (5), 574–581.

Xu, L., Groth, K.M., Pearlson, G., Schretlen, D.J., Calhoun, V.D., 2009. Source-based morphometry: the use of independent component analysis to identify gray matter differences with application to Schizophrenia. Hum. Brain Mapp. 30 (3), 711–724.

Xydakis, M.S., Dehgani-Mobaraki, P., Holbrook, E.H., Geisthoff, U.W., Bauer, C., Hautefort, C., Herman, P., Manley, G.T., Lyon, D.M., Hopkins, C., 2020. Smell and taste dysfunction in patients with COVID-19. Lancet Infect. Dis. 20 (9), 1015–1016.

Yavarpour-Bali, H., Ghasemi-Kasman, M., 2020. Update on neurological manifestations of COVID-19. Life Sci. 257, 118063.

Zhang, H., Wang, X., Lin, J., Sun, Y., Huang, Y., Yang, T., Zheng, S., Fan, M., Zhang, J., 2013. Reduced regional gray matter volume in patients with chronic obstructive pulmonary disease: a voxel-based morphometry study. AJNR Am. J. Neuroradiol. 34 (2), 334–339.